DOI 10.1007/s11595-015-1158-x

Phase Morphology Evolution in AISI301 Austenite Stainless Steel under Different Cooling Rates

BAI Liang[1], MA Yonglin[2*], XING Shuqing[2], LIU Chenxin[3], ZHANG Jieyu[1]

(1. Shanghai Key Laboratory of Modern Metallurgy and Materials Processing, Shanghai University, Shanghai 200072, China; 2. Material and Metallurgical School, Inner Mongolia University of Science and Technology, Baotou 014010, China; 3. Jinan Iron and Steel Co., Ltd. Jinan 250101, China)

Abstract: Quenching experiments were performed at different cooling rates under non-directional solidification by differential thermal analysis, and the morphologic variation of primary phase, phase transition temperature and hardness change at the same quenching temperature were investigated. The experimental results show that, with the gradual decrease of the cooling rate from 25 K/min, the morphology of ferrite starts to transform experiencing the dendrite, radial pattern, Widmanstatten-like and wire-net. Sample starts to present the Widmanstatten-like microstructure at 10 K/min which does not exist at higher or lower cooling rates, and this microstructure is detrimental to the mechanical property. Except 10 K/min, the hardness decreases with decreasing cooling rate.

Key words: cooling rate; non-directional solidification; morphology evolution; primary phase

1 Introduction

The structural and functional material of peritectic alloy system is rapidly developed as Fe-Cr-Ni stainless steel[1,2], high-temperature structural material with important application prosperity as Ti-Al, Fe-Al, Ni-Al system[3-7], YBCO high-temperature superconducting material[8] and Nd-Fe-B magnetic material[9]. In the above metal solidification investigation, it is found that the precipitation morphology of the primary phase plays an important role in the solid phase transition, the final microstructure and the mechanical property. Material property could be obviously improved by phase transition control along with the application field broaden which is urgent to deeply understand the change law of the phase precipitation morphology in the solidification.

Solidification investigation at present is mostly focused on directional solidification process microstructure transition and phase selection of the new advanced material[10-12], but less focused on non-directional solidification research. Nassar H *et al*[13] studied the low alloy steel with variable alloy content by differential thermal analysis(DTA) and found that with the reduction of the carbon content or increase of the molybdenum content, the difference of temperature between liquidus and peritectic reaction will increase during the solidification process, meanwhile, the cooling rate has less impact on the growth of the austenite. Dhindaw[14] investigated the peritectic reaction of the medium-alloy steel by DTA, and indicated how to divide the area of peritectic reaction from the area that the austenite directly nucleated by liquid phase through the research of the energy release analysis and the microstructure segregation of Cr and Ni.

In this work, quenching experiment on AISI 301 austenite stainless steel was performed at different cooling rates by DTA method, and the morphology change of primary phase, the phase transition temperature variation and the quenching hardness variation were discussed.

(Received: Apr. 5, 2014; Accepted: June 10, 2014)

BAI Liang (白亮): Ph D Candidate; E-mail:bailiang410@163.com

*Corresponding author: MA Yonglin(麻永林): Prof.; Ph D; E-mail: malin@imust.cn

Funded by the National Natural Science Foundation of China(No. 2010DFB70630)

2 Experimental

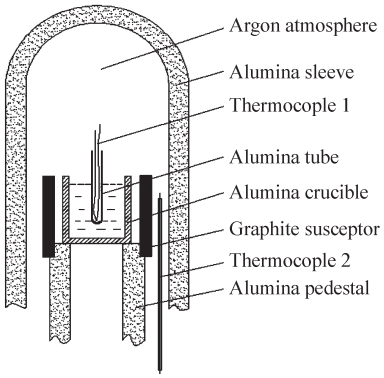

Fig.1 The heat and cooling area of sample in DTA

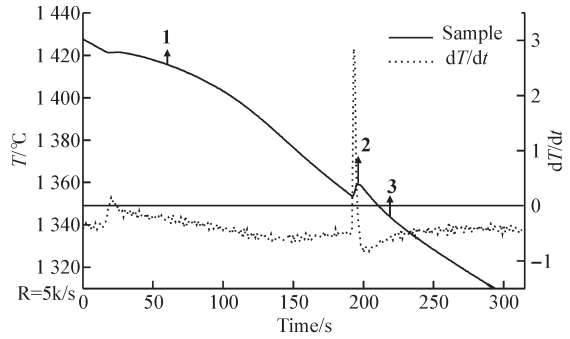

Fig.2 Thermal analysis curve of austenite stainless steel

The chemical composition of the AISI 301 stainless sample in this study (mass fraction, %) was as follows: C 0.078, Cr 17.03, Ni 7.16, Si 0.48, Mn 1.07, P 0.032, S 0.016, Fe remaining amount. Fig.1 is a sectional diagram of the heat and cooling area for sample in DTA. DTA sample was cylindrical with 8 mm diameter and 13 mm height, as well as a small hole longitudinally drilled in the circle center of the sample with 1mm diameter and 6 mm depth for the thermal couple 1 to measure temperature of the sample. Thermal couple 2 was for the temperature measurement inside the furnace. Of all the DTA equipment, the two thermal couples used for the temperature measurement were both platinum-rhodium alloy, with the temperature data recorded by a high frequency recorder as for the foundation of temperature-time curve. Fig.2 is the thermal analysis curve for 301 austenite stainless steel. In Fig.2, **1** is the precipitation of primary δ ferrite at 1 688 K, **2** is the precipitation of the γ austenite in peritectic reaction at 1 632 K, **3** is the end of solidification at 1 619 K. The experiment procedure was as follows according to the temperature curve: the metal was heated at 1 723 K to melt and cooled down at the rate of 25, 15, 10, 4 K/min to 1 688 K, then quenched in water together with the crucible. Ferrite, austenite and the residual liquid phase were all kept to the room temperature, and the morphology of primary precipitation in the solidification process can be observed by optical microscope.

Sample was cut vertically, put into an artificial resins holder, then polished and corroded. The etching solution is 12% hydrochloric acid, 8% nitric acid and 80% water. Fig.3 is the different microstructural morphology at different cooling rates with the precipitation of the primary phase, which shows the impact of cooling rate on the process of precipitation for primary phase. Fig.4 is the enlarged drawing of the precipitation microstructure for analysis of the precipitated transformation law with the change of cooling rate. Fig.5 is the microstructure when the temperature cooled down to room temperature at 25 K/min, the structure variation is analyzed from the precipitation to the final microstructure at room temperature.

3 Results and discussion

3.1 Morphologic evolution of primary phase

In the metal or alloy solidification, the main aspect affecting the solidifying process and microstructure is the alloy composition and cooling condition. To simplify the influence of each alloy element to austenite stainless solidification, the conversion from the alloy element influence to the Cr/Ni equivalent simplifies the complex alloy composition into the ternary alloy Fe-Cr-Ni, the solidification of austenite stainless steel is divided into four models as to the Cr_{eq} and Ni_{eq} [15]. In this article, the solidification sequence is followed as the model $L\rightarrow(L+\delta)\rightarrow(L+\gamma+\delta)\rightarrow(\gamma+\delta)$ within the overcooling scope range. δ phase which is considered as the primary phase, is first precipitated from the liquid at the process of alloy solidification, with the reason that the nucleation driven force (the volume free energy difference of solid and liquid phase) of δ phase is larger than that of γ phase, with less nucleation resistance (interfacial energy between solid and liquid phases). However, morphology of primary phase for Fe-Cr-Ni alloy will still has big change as to the difference cooling rate. Different from the single morphologic microstructure under the condition of directional solidification with the constant cooling rate, temperature gradient and the growth rate, the microstructure appears with complex diversity under the condition of non-directional solidification, however, the change law of the morphology can clearly be found.

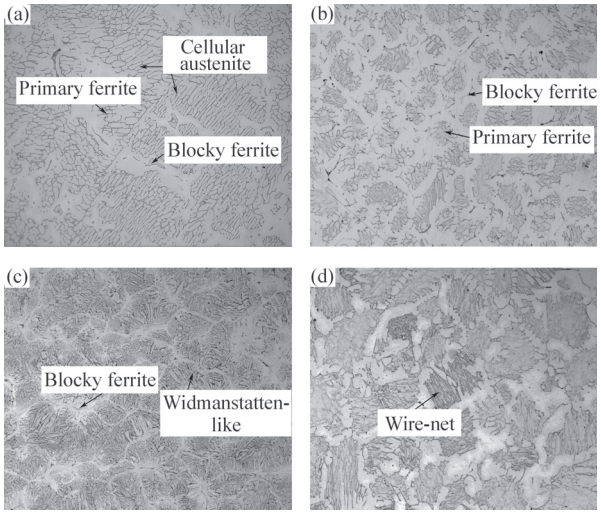

Fig.3 Microstructure images of quenched sample at 1 688 K at different cooling rates (100×): (a) 25 K/min; (b) 15 K/min; (c) 10 K/min; (d) 4 K/min

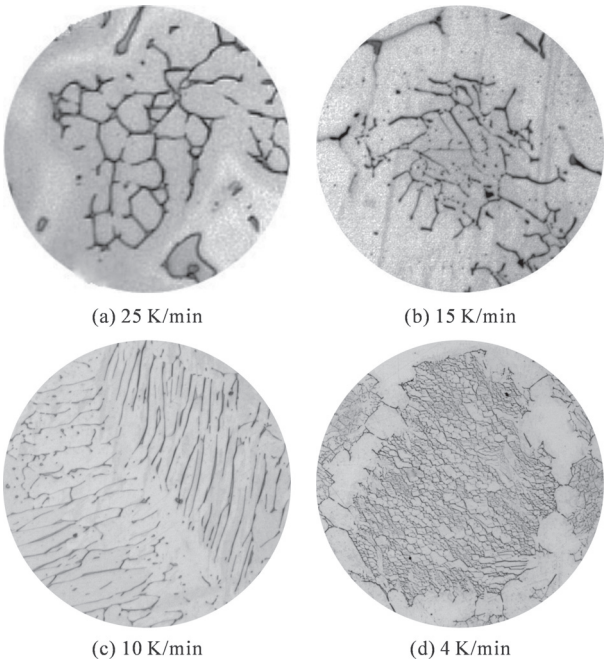

Fig.4 Morphology change of ferrite at different cooling rates

Fig.3 is the microstructure shape of quenched sample at different cooling rates, and Fig.4 is the partial enlarged diagrams of ferrite phase. It is shown in Fig.3(a) that dendritic ferrite is floated in liquid phase as tiny dendritic island, and most of residual liquid phase forms the cellular austenite after quenching. Liang *et al*[16] found out by in-situ observation to the δ-γ phase transition of AISI 304 austenite stainless steel, the γ phase shows as developed large dendrite in the liquid with 24 K/min cooling rate. The primary precipitated ferrite from liquid phase has already formed the frame, and the austenite precipitates out and surrounds the ferrite while the peritectic reaction happens. It filled into the space between dendritic ferrite that is shown as large dendritic γ phase after the temperature reduces below the peritectic temperature.

Primary δ ferrite in liquid phase exists as the short dendrite, with the meaning that the dendritic ferrite shown in Fig.4(a) only exists inside the sample before quenching, and the remaining area is liquid. During the process of quenching, part of liquid phase quickly forms the cellular austenite shown in Fig.3(a) and the thin bars of ferrite were precipitated between these cellular austenitic. As well as the nucleation and growth of the cellular austenite, large amount of Cr enriched into the small part of liquid where the last solidification part liquid eventually solidified to the blocky ferrite shown in Fig.3(a). In the normal continuous solidification, this part of blocky ferrite will not exist in the microstructure under this temperature, which should be a part of liquid, so it could be considered as the liquid phase during the microstructure analysis before the quenching. The ferrite existed in the final microstructure of austenite stainless steel is not this part ferrite retaining. It is because that sample steps into the solid phase transition after the temperature decreased below the solidus, solute diffusion caused by the austenite growth makes part of austenite area unstable. With the increase of instability, tiny ferrite appears inside austenite, and the instability of tiny ferrite will increase with the temperature decreasing. This tiny ferrite grows as blocky ferrite by element diffuse during the solidified process, which is the blocky microstructure at room temperature, as shown in Fig.5. It is the microstructure at room temperature at the rate of 25 K/min.

With the cooling rate decreasing to 15 K/min as shown in Fig.3(b), ferrite gradually precipitated out and uniformly distributed in the liquid phase independently. Large area of liquid phase no longer existed independently in the samples. The morphology of ferrite is transformed from the dendrite as shown in Fig.4(a) to radial pattern in Fig.4(b). Arms of ferrite stretch into the liquid, and gradually grow until contact each other in the solidified process. Liquid between the ferrite arms is directly solidified to austenite in the quenching process. The ferrite precipitation from liquid phase is distributed in the whole liquid phase area like small islands. Distance between islands is short without large range of independent liquid area, and it can not form the cellular austenite area during the quenching process. However, the last solidified liquid surrounded by the ferrite and austenite also precipitated to the narrow and long blocky ferrite by the element

segregation in the solidification process as shown in Fig.3(b).

Fig.3(c) is the microstructure at the cooling rate of 10 K/min, from the whole figure of view, the parallel ferrite fills in the whole solidified area, island gap is narrow owing to the parallel ferrite precipitation and growth, remaining the few liquid phases. From the enlarged microstructure diagram (Fig.4(c)), the morphology of primary ferrite is very similar to the classic Widmanstatten microstructure, so it is named as Widmanstatten-like ferrite. According to the investigation of Widmanstatten microstructure, it was found that it exists in the sample center at low cooling rate, and it is harmful to the strength of the material. For a specific type of alloy, increase or decrease of the cooling rate can reduce or avoid the formation of Widmanstatten structure. In this paper, the Widmanstatten-like microstructure exists at the low cooling rate (10 K/min) under non-directional condition, there is no similar microstructure when the cooling rate is higher or lower than 10 K/min, which indicates that the primary phase will precipitate out the Widmanstatten-like microstructure when the austenite stainless steel solidified at 10 K/min under non-directional condition.

Fig.3(d) is the microstructure cooling at 4 K/min, which shows that the ferrite dissociates in liquid phase as the wire clusters, and these wire clusters are connected with each other by the coarse ferrite. There is no obvious blocky ferrite transition in the quenching microstructure, because the primary ferrite islands distribute uniformly and mutually connected, which divide the liquid into small partial area with the result of the quick formation of the austenite between the wire cluster area in the quenching process. These small areas of liquid are not easy to enrich the elements and to directly transform as blocky ferrite. It is shown in Fig.4(a) which is enlarged diagram of primary ferrite that the parallel growth of wire ferrite entangles two side of wire, and knits the diamond net ferrite microstructure. This microstructure under the non-directional solidification condition is first observed which is named as wire-net ferrite.

From the above discussion, the precipitation morphology of ferrite will be different from each other. With the decrease of the cooling rate, the dendritic ferrite stretches smoothly into the liquid phase, as well as transform experienced radial pattern, Widmanstatten-like and wire-net.

3.2 Variation of strength and phase transition temperature

It is revealed that phase transition of stainless steel in process of solidification plays very important role in the property. The resistance ability of thermal crack for alloy as primary ferrite is stronger than as primary austenite. The diffusion rate inside ferrite is approximate 100 times higher than inside austenite for the alloy elements. When the stainless steel takes the ferrite as the primary phase, alloy elements and harmful microelement such as P, S distribute uniformly in the dendritic crystal, so the mechanical property is uniform with the good plastical toughness and high hardness[17,18]. The three values of Rockwell hardness of samples were measured in center of the cylindrical sample, middle of the radius and the edge, to give the average values which are listed in Table 1.

Table 1 Average hardness change in the solidifying process

Parameter	25 K/min	15 K/min	10 K/min	5 K/min
Hardness/HRC	57.5	56	45.75	51
Strength/(N/mm^2)	2 145	2 050	1 504	1 740

Note: hardness and tensile strength contrast to the German standard DIN50150

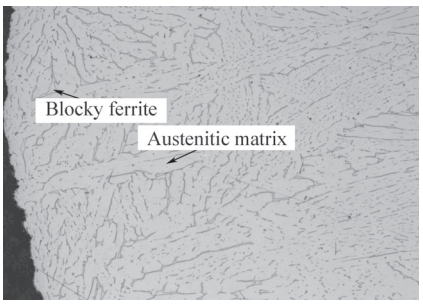

Fig.5 Microstructure at room temperature of 25 K/min; magnification:100 times

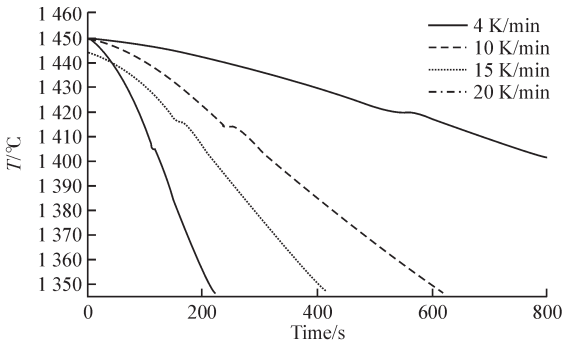

Fig.6 Precipitation temperature variation of primary phase

It is shown in Table 1 that except at 10 K/min, samples hardness at 1 688 K increases with increasing cooling rate. With regards to the 10 K/min cooling rate, hardness is obviously lower than that of the other samples, caused by precipitation of the large

amount of Widmanstatten-like microstructure in this range of cooling rate, which makes the hardness of quenched sample drop down evidently. As we know, the Widmanstatten microstructure will affect the mechanical property of the steel, especially decrease the plasticity and affect toughness and increase the brittle transition temperature. The Widmanstatten-like microstructure has the same property to reduce hardness of the cast. It is harmful to mechanical property, so in the process of cast production, this microstructure should be avoided in material.

The impact of cooling rate on phase transition temperature is relatively simple. The bigger the overcooling of liquid will bring the lower transition temperature. With the decrease of the cooling rate, the process is more close to equilibrium solidification, and the temperature of phase precipitation is almost not changed. Therefore, the impact of cooling rate on phase transformation could be ignored when cooling rate decreases to some degree. From Fig.6, it can be seen that the temperature change caused by the primary phase will stay in 1 678 K when cooling rate is 25 K/min, and 15 K/min, 10 K/min, 4 K/min will be respectively matched with 1 690 K, 1 688 K, 1 692 K. Under the condition of non-directional solidification, the precipitation temperature of primary phase will increase with decreasing cooling rate, however, the temperature change becomes less when the cooling rate is below 15 K/min. Cooling rate is no longer the main aspect to the phase transition temperature.

4 Conclusions

a) Under the condition of non-directional solidification, the morphology of primary phase in cylindrical sample transforms from dendritic crystal to radial shape, Widmanstatten-like and finally the wire-net. The dendritic ferrite gradually stretches to parallel by changing the angle.

b) AISI301 austenite stainless steel shows the Widmanstatten-like microstructure when cooling rate is 10 K/min under non-directional solidification. There is no such similar microstructure when the cooling rate is higher or lower than this cooling rate.

c) The Widmanstatten-like microstructure appeared at 10 K/min is detrimental to the mechanical property, which should be avoided in such cooling rate range. In addition to the sample which has Widmanstatten-like microstructure, the hardness of other quenching samples gradually decreases with decreasing cooling rate.

Acknowledgements

The authors express their appreciation to Professor Fredriksson H (KTH) for his valuable comments during the course of this work.

References

[1] Umeda T, Okane T, Kurz W. Phase Selection During Solidification of Peritectic Alloys[J]. *Acta Mater.*, 1996, 44: 4 209-4 216

[2] Arai Y, Emi T, Fredriksson H, *et al. In-situ* Observed Dynamics of Peritectic Solidification and δ/γ Transformation of fe-3 to5 at. Pct in Alloys[J]. *Metall Trans. A*, 2005, 36: 3 065-3 074

[3] Kim MC, Oh MH, Lee JH, *et al.* Composition and Growth Rate Effects in Directionally Solidified Tial Alloys[J]. *Sci. Eng. A*, 1997, 240: 570-576

[4] Busse P, Meissen F. Coupled Growth of the Properitectic α-and the Peritectic γ-Phases in Binary Titanium Aluminides[J]. *Scr Mater*., 1997, 36: 653-658

[5] Vandyoussefi M, Kerr HW, Kurz W. Two-Phase Growth in Peritectic Fe-Ni Alloys[J]. *Acta Mater.*, 2000, 48(9): 2 297-2 306

[6] Lee JH, Verhoeven JD. Characteristics of Crystal Growth from Solution: Scaling Laws[J]. *Cryst. Growth*., 1994, 144(3-4):353-366

[7] Lapin J, Klimova A, Velisek R, *et al.* Directional Solidification of Ni-Al-Cr-Fe Alloy[J]. *Scripta Mater*., 1997, 37(1): 85-91

[8] W Lo, Cardwell DA, Dewhurst CD, *et al.* Fabrication of Large Grain YBCO by Seeded Peritectic Solidification[J]. *Mater. Res*., 1996, 11(4): 786-794

[9] Fidler J, Schrefl T. Overview of Nd-Fe-B Magnets and Coercivity (invited)[J]. *Journal of Applied Physics*, 1996, 79(8): 5 029-5 034

[10] Hunter A, Ferry M. Phase Formation during Solidification of AISI 304 Austenitic Stainless Steel[J]. *Scripta Mater*., 2002, 46: 253-258

[11] Umeda T, Okane T, Kurz W. Phase Selection during Solidification of Peritectic Alloys[J]. *Acta Mater*., 1996, 44: 4 209-4 216

[12] Fukumoto S, Okane T, Umeda T, *et al.* Crystallographic Relationships between Ferrite and Austenite during Unidirectional Solidification of Fe-Cr-Ni Alloys[J]. *ISIJ Int*., 2000, 40(7): 677-684

[13] Nassar H, Fredriksson H. Metallurgical and Materials Transactions A-Physical Metallurgy and Materials Science[J]. *Metall. Mater. Trans. A*, 2010, 41A: 2 776-2 783

[14] Dhindaw BK, Antonsson T, Tinoco J, *et al.* Characterization of the Peritectic Reaction in Medium-Alloy Steel through Microsegregation and Heat-of-Transformation Studies[J]. *Metall Mater Trans. A*, 2004, 35A: 2 869-2 879

[15] Rajasekhar K, Harendranath CS, Raman R, *et al.* Microstructural Evolution during Solidification of Austenitic Stainless Steel Weld Metals: A Color Metallographic and Electron Microprobe Analysis Study[J]. *Materials Characterization*, 1997, 38(2): 53-65

[16] Liang GF, Zhou WC, Nolli P, *et al. In Situ* Observation of Nucleation and Growth of High-Temperatureδphase in Stainless Steel AISI 304 during Heating[J]. *Acta Metal Sin.*, 2006, 42(8): 805-809

[17] Fukumoto S, Kurz W. Prediction of the δ to γ Transition in Austenitic Stainless Steels during Laser Treatment[J]. *ISIJ Int*., 1997, 37(7): 677-684

[18] Brooks JA, Thompson AW. Microstructural Development and Solidification Cracking Susceptibility of Austenitic Stainless Steel Welds[J]. *Int. Mater. Rev*., 1991, 36(1): 16-44